Structural Modulation of the Dipolar−Octupolar Contributions to the NLO Response in Subphthalocyanines

Christian G. Claessens,[†] David González-Rodríguez,[†] Tomás Torres,*[,†] Guillermo Martín,[‡,§] Fernando Agulló-López,[‡] Isabelle Ledoux,[§] Joseph Zyss,*[,§] Victor R. Ferro,[||] and José M. García de la Vega*[,||]

Departamento de Química Orgánica (C-I), Departamento de Física de Materiales (C-IV), and Departamento de Química-Física Aplicada (C-XIV), Universidad Autónoma de Madrid, 28049-Madrid, Spain, and Laboratoire de Photonique Quantique et Moléculaire, Ecole Normale Supérieure de Cachan, 94235 Cachan, France

Received: October 13, 2004; In Final Form: December 10, 2004

Second order nonlinear optical properties of a series of trinitrosubphthalocyanine (SubPc) isomers were studied experimentally by electric field induced second harmonic (EFISH) generation and hyper Rayleigh scattering (HRS). These experimental values were compared to the ones obtained theoretically employing both sum over states (SOS) and finite field (FF) methods. From these studies, it was shown that the dipolar contributions to the β tensor are very much dependent on the substitution pattern at the periphery of the subphthalocyanine macrocycle, whereas the octupolar contributions remain mostly unchanged. Consequently, it was deduced that SubPc is extremely well suited for the decoupling of octupolar and dipolar contribution to the NLO response.

Introduction

The nonlinear optical (NLO) properties of organic compounds are of great relevance in the continuously evolving fields of optoelectronics and photonics.[1] High dipolar NLO responses have been observed in the so-called "push−pull" molecules, in which a permanent dipole moment provides ground state charge asymmetry that may be redistributed, under the influence of an electric field, through a highly polarizable π-conjugated system.[2] On the other hand, it was shown experimentally and theoretically that an octupolar charge distribution, when integrated within a polarizable framework, may also contribute significantly to the NLO behavior of organic molecules.[3,4] Many organic compounds possess dipolar and octupolar characters, and both play a part in their overall NLO behavior. Recently, the NLO responses of strongly octupolar three-dimensional π-conjugated molecules and metal−ligand complexes have been studied,[5−7] among which subphthalocyanines (SubPcs, Figure 1)[8−10] represent a singular example. Previous studies demonstrated the influence of the nature of the SubPc substituents on the strength of its quadratic NLO response, showing that electron-withdrawing peripheral substituents tend to improve its first-order hyperpolarizability.[11] This cone-shaped molecule provides an ideal tool for studying at the same time its dipolar and octupolar character, since it possesses not only a permanent dipole moment along its B−Cl bond but also an octupolar charge distribution within its highly polarizable three-dimensional aromatic system.

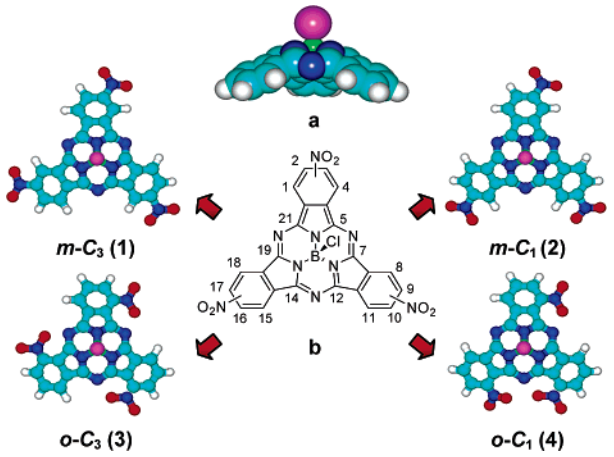

Figure 1. (a) Cone-shaped structure of SubPcs. (b) Structure of the four SubPc isomers **1**−**4**.

In this article we describe in a first instance the synthesis, separation and characterization of a series of four structural isomers (**1**−**4**, Figure 1) of trinitro-substituted subphthalocyanine, namely the C_3- and C_1-symmetrical isomers of the ortho-[12] and meta-substituted subphthalocyanine derivatives.[13] Their second order nonlinear optical properties were measured experimentally employing both hyper Rayleigh scattering[14−16] (HRS) and electric field induced second harmonic generation[17,18] (EFISH) techniques. Moreover, second order nonlinear optical parameters were also derived theoretically by means of both the sum over states[19] (SOS) and the finite field[20] (FF) methods using the structures optimized by the density functional theory (DFT). The components of the hyperpolarizability tensors computed in this manner allowed us to calculate the relative amplitude of dipolar ($\beta^{J=1}$) and octupolar ($\beta^{J=3}$) hyperpolarizabilities of the studied compounds as defined in spherical coordinates. In this form, the influence of the substitution pattern

* To whom correspondence should be addressed. E-mail: (T.T.) tomas.torres@uam.es; (J.Z.) zyss@lpqm.ens-cachan.fr; (J.M.G.d.l.V.) delavega@uam.es.

[†] Departamento de Química Orgánica (C-I), Universidad Autónoma de Madrid.

[‡] Departamento de Física de Materiales (C-IV), Universidad Autónoma de Madrid.

[§] Ecole Normale Supérieure de Cachan.

[||] Departamento de Química-Física Aplicada (C-XIV), Universidad Autónoma de Madrid.

10.1021/jp045322u CCC: $30.25
Published on Web 02/15/2005

on the dipolar to octupolar NLO response ratio was unambiguously determined.

Experimental Section

General Procedures. UV/vis spectra were recorded with a Hewlett-Packard 8453 instrument. IR spectra were recorded on a Bruker Vector 22 spectrophotometer. LSI-MS and HRLSI-MS spectra were determined on a VG AutoSpec instrument. NMR spectra were recorded with a BRUKER AC-300 instrument. Elemental analyses were performed with a Perkin-Elmer 2400 apparatus. Column chromatographies were carried out on silica gel Merck-60 (230−400 mesh, 60 Å), and TLC on aluminum sheets precoated with silica gel 60 F_{254} (E. Merck). Chemicals were purchased from commercial suppliers and used without further purification. ***o*-C_3** (**3**) and ***o*-C_1** (**4**) were synthesized according to a previously described procedure.[12]

General Synthetic Procedure for the Synthesis of SubPcs *m*-C_3 (1) and *m*-C_1 (2). In a 25 mL two-necked round-bottomed flask, equipped with a condenser, magnetic stirrer, and rubber seal, was added BCl_3 (5 mL, 1 M solution in *p*-xylene) to dry 4-nitrophthalonitrile (0.86 g, 5 mmol) under argon atmosphere. The reaction mixture was then stirred under vigorous reflux for 15 min, allowed to reach room temperature, and flushed with argon. The dark purple reaction slurry was dissolved in toluene/THF (10:1) and passed through a short silica plug. The solvent was removed by vacuum distillation, and the resulting dark magenta solid was subjected to column chromatography on silica gel using toluene/THF (20:1) as eluent in order to separate the C_3 (**1**) and C_1 (**2**) regioisomers. Each compound was further purified by precipitation and filtration from hexane/CH_2Cl_2, obtaining dark magenta solids listed below following their elution order.

*Chloro-[2,9,16-trinitro-7,12:14,19-diimino-21,5-nitrilo-5H-tribenzo[c,h,m][1,6,11] triazacyclopentadecinato-(2)-κN^{22},κN^{23},κN^{24}]-boron(III) (**m-C_3, 1**).* Yield: 23%. Mp > 250 °C. ^{1}H NMR (300 MHz, $CDCl_3$): δ (ppm) = 9.78 (d, J_m = 2.0 Hz, 3H; H-1, H-8, H-15), 9.08 (d, J_o = 8.5 Hz, 3H; H-4, H-11, H-18), 8.86 (dd, J_o = 8.5 Hz, J_m = 2.0 Hz, 3H; H-3, H-10, H-17). ^{13}C NMR (75.5 MHz, $CDCl_3$): δ (ppm) = 150.6, 149.6 (6C; C-5, C-7, C-12, C-14, C-19, C-21), 149.2 (3C; C-2, C-9, C-16), 134.3 (3C; C-4a, C-11a, C-18a), 131.0 (3C; C-7a, C-14a, C-21a), 125.6 (3C; C-3, C-10, C-17), 123.9 (3C; C-4, C-11, C-18), 119.0 (3C; C-1, C-8, C-15). The low solubility of this product prevented the obtention of a ^{13}C NMR spectrum with better resolution. MS (LSI-MS, *m*-NBA): *m/z* = 565 $[M]^+$ (10%). HRLSI-MS ($C_{24}H_{10}N_9O_6BCl$) $[M + H]^+$: calcd, 565.0536; found, 565.0531. UV−vis ($CHCl_3$): λ_{max} (nm) (log ϵ (dm^3 mol^{-1} cm^{-1})) = 581 (4.7), 533 (sh), 306 (4.3). FT-IR (KBr), ν (cm^{-1}): 3094, 1619, 1605, 1528 (NO_2, asym), 1464, 1398, 1341, and 1314 (NO_2, sym), 1260, 1233, 1179, 1139, 1102, 1085, 980 (B−Cl), 909, 857, 805, 741, 701. Anal. Calcd ($C_{24}H_9N_9O_6BCl$): C, 50.96; H, 1.60; N, 22.29. Found: C, 50.91; H, 1.65; N, 22.27.

*Chloro-[2,9,17-trinitro-7,12:14,19-diimino-21,5-nitrilo-5H-tribenzo[c,h,m][1,6,11] triazacyclopentadecinato-(2)-κN^{22},κN^{23},κN^{24}]-boron(III) (**m-C_1, 2**).* Yield: 65%. Mp > 250 °C. ^{1}H NMR (300 MHz, $CDCl_3$): δ (ppm) = 9.79 (d, J_m = 2.0 Hz, 2H; H-1/H-8/H-18), 9.78 (d, J_m = 2.0 Hz, 1H; H-1/H-8/H-18), 9.08 (d, J_o = 8.5 Hz, 1H; H-4/H-11/H-15), 9.06 (d, J_o = 8.5 Hz, 2H; H-4/H-11/H-15), 8.88 (dd, J_o = 8.5 Hz, J_m = 2.0 Hz, 1H; H-3/H-10/H-16), 8.854 (dd, J_o = 8.5 Hz, J_m = 2.0 Hz, 1H; H-3/H-10/H-16), 8.847 (dd, J_o = 8.5 Hz, J_m = 2.0 Hz, 1H; H-3/H-10/H-16). ^{13}C NMR (75.5 MHz, $CDCl_3$): δ (ppm) = 150.8, 150.6, 150.2, 150.1, 150.0, 149.6 (6C; C-5, C-7, C-12, C-14, C-19, C-21), 149.4, 149.3, 149.1 (3C; C-2, C-9, C-16), 134.3, 134.1, 133.7 (3C; C-4a, C-11a, C-14a), 131.2, 131.0, 129.8 (3C; C-7a, C-18a, C-21a), 125.7, 125.5, 125.4 (3C; C-3, C-10, C-16), 123.8, 123.7 (3C; C-4, C-11, C-15), 119.0, 118.9 (3C; C-1, C-8, C-18). MS (LSI-MS, *m*-NBA): *m/z* = 565 $[M]^+$ (12%). HRLSI-MS ($C_{24}H_{10}N_9O_6BCl$) $[M + H]^+$: calcd, 565.0536; found, 565.0535. UV−vis ($CHCl_3$): λ_{max} (nm) (log ϵ (dm^3 mol^{-1} cm^{-1})) = 588 (4.5), 569 (4.5), 532 (sh), 523 (sh), 302 (4.4). FT-IR (KBr), ν (cm^{-1}): 3101, 1622, 1586, 1530 (NO_2, asym), 1462, 1397, 1341, and 1327 (NO_2, sym), 1260, 1233, 1179, 1139, 1058, 984 (B−Cl), 909, 857, 843, 801, 753, 699. Anal. Calcd ($C_{24}H_9N_9O_6BCl$): C, 50.96; H, 1.60; N, 22.29. Found: C, 50.82; H, 1.72; N, 22.18.

Electric Field Induced Second Harmonic (EFISH) Generation Measurements.[17,18] NLO dipolar molecules are oriented in solution using a dc electric field $E°$ (or, more precisely, a pulsed field with adjustable microsecond to millisecond time-plateau synchronized with the fundamental nonosecond laser pulse). The coherently emitted second harmonic signal from the oriented solution is proportional to $N^2\langle\beta\rangle^2 \sin^2 l/l_c$ where l is the optical pathway through the solution and l_c the coherence length of the second harmonic generation process. The $\mu\cdot\beta$ value of the investigated chromophore can then be inferred from the amplitude and period of the resulting so-called "Maker fringes" obtained by moving an edge-shaped cell containing a solution of the investigated molecule along a direction perpendicular to the incident laser beam and the dc poling field. The SHG signal from the solution is compared to that of a reference compound, usually the pure solvent.

As the EFISH experiment is based on coherent second harmonic generation, the resulting SHG signals are usually easily detectable; fundamental wavelengths as long as 1.91 μm (as generated from an hydrogen Raman shifting cell pumped at 1.06 μm) can be used, then allowing for reliable results even for molecules that display a wide and red-shifted electronic absorption spectrum in the visible range.

EFISH experiments of the four isomers have been performed in chloroform solution at similar concentrations (***m*-C_3** (**1**), 1.8 × 10^{-3} M; ***m*-C_1** (**2**), 1.1 × 10^{-3} M; ***o*-C_3** (**3**), 0.7 × 10^{-3} M; ***o*-C_1** (**4**), 0.6 × 10^{-3} M) at 1.907 μm fundamental wavelengths. It was obtained by shifting the 1.064 emission of a Q-switched Nd:YAG laser in a high-pressure hydrogen cell (60 bar). A peak power density of 1.26 × 10^{11} W/cm^2 was achieved with pulses of 10 ns duration and 10 Hz repetition rate. The incident beam was synchronized with a dc voltage pulse applied periodically in order to break its centrosymmetry while avoiding charge deposition on the electrodes.

Hyper-Rayleigh Scattering (HRS) or Harmonic Light Scattering (HLS) Measurements.[14−16] HRS or HLS experiments had been implemented in the earliest nonlinear optical studies (Maker and Terhune, see ref 14), but had been somehow superseded by EFISH in view of the dominance of the dipolar scheme. It has been revived in the current context to provide adequate and relatively easy measurements techniques of octupolar β's. Noncoherent HRS experiments performed in centrosymmetric solutions allow indeed to retrieve some basic tensorial features of the β tensor for multipolar molecules of interest. The nonlinear effect in HRS originates from orientational fluctuations of the scattering centers, leading to a NLO response proportional to the orientationally averaged $\langle\beta\otimes\beta\rangle$ quantity. The experimental setup is derived from that initially proposed by Terhune and Maker.[14] In our configuration, the determination of the $\langle\beta\otimes\beta\rangle$ quantity is inferred from the slope

of the scattered second harmonic light plotted as a function of a "monitoring" SHG signal (emitted by a frequency doubling powder like NPP, for example). The incident fundamental laser beam can vary continuously by rotating a half-wave plate between two crossed polarizers. The scattered harmonic signal is collected at 90° with respect to the incident beam using a set of converging lenses, and sent into a photomultiplier. As for EFISH measurements, HLS measurements are carried-out on solutions of the investigated molecules at various concentrations, and compared to the HLS signal of a "reference" liquid, ca. the pure solvent.

The HRS experiments were carried out by measuring the intensity of the scattered second-harmonic light generated when focusing the intense 1.34 μm laser beam on the centrosymmetric solution. Harmonic emission was registered in perpendicular direction and no indication of multiphoton-induced fluorescence was obtained from our experiments, since signal slightly out of the 2ω was very weak, as checked with several narrow-band interferential filters. The following concentrations were employed: ***m*-C_3 (1)**, 2.1×10^{-4} M; ***m*-C_1 (2)**, 1.3×10^{-4} M; ***o*-C_3 (3)**, 2.5×10^{-4} M; ***o*-C_1 (4)**, 1.9×10^{-4} M.

Calculations. Four structures corresponding to the *o*- and *m*-nitro-substituted derivatives of the SubPc in their C_1 and C_3 point groups of symmetry have been computed. The calculations included full geometry optimization. The DFT methods were selected for both the geometry optimization and the electronic structure characterization of the ground electronic state of these molecules. The hybrid functional B3LYP[21,22] and the 6-31G-(d,p)[23] basis sets were employed. The DFT calculations were computationally supported by the Gaussian98 program package.[24]

The molecular hyperpolarizabilities of the studied molecules were calculated by two parallel theoretical approaches: (i) the finite field (FF) method[20] and (ii) the sum over states (SOS) formalism.[19]

In the FF procedure,[20] the permanent dipole moment (μ) of a molecule in its ground electronic state, in the presence of a static external field (E), is expanded as a Taylor series:

$$\mu_{induced} = \mu_i + \alpha_{ij}\cdot E + {}^1/_{2!}\cdot\beta_{ijk}\cdot E\cdot E + {}^1/_{3!}\cdot\gamma_{ijkl}\cdot E\cdot E\cdot E \quad (1)$$

The tensor components of the molecular polarizability (α_{ij}) and hyperpolarizabilities (β_{ijk} and γ_{ijkl}) can be calculated by taking the appropriate derivatives of the total electronic energy or dipole moment with respect to the external field:

$$\mu_i = \frac{\partial U}{\partial E_i};\ \alpha_{ij} = \frac{\partial \mu_i}{\partial E_i};\ \beta_{ijk} = \frac{\partial^2 \mu_i}{\partial E_j \partial E_k}$$

and

$$\gamma_{ijkl} = \frac{\partial^3 \mu_i}{\partial E_j \partial E_k \partial E_l} \quad (2)$$

In the present work, the FF procedure was employed as implemented in the Gaussian98 program package. The computational method and the basis sets selected in this work guarantee an adequate accuracy of the calculated hyperpolarizabilities. The DFT methods take into account the electron correlation in an implicit and computational expedient manner whereas the 6-31G(d,p) basis sets include the polarization functions, both needed for an adequate theoretical description of the NLO properties of porphyrine-based systems.[21−23,25,26]

In the SOS procedure,[19] the theoretical description of hyperpolarizability tensors β_{ijk} and γ_{ijkl} requires a three level model. Within this formalism, the more general expression for β_{ijk} is given by

$$\beta_{ijk} = \beta_{ijk}(2lev,|1\rangle + \beta_{ijk}(2lev,|2\rangle + \frac{1}{\hbar^2}[\mu^i_{01}(\mu^j_{12}\mu^k_{02} + \mu^j_{02}\mu^k_{12})D^{(a)}_{12} + \mu^i_{02}(\mu^j_{12}\mu^k_{01} + \mu^j_{01}\mu^k_{12})D^{(a)}_{21} + \mu^i_{12}(\mu^j_{02}\mu^k_{01} + \mu^j_{01}\mu^k_{02})D^{(b)}_{12}] \quad (3)$$

where

$$\beta_{ijk}(2lev,|n\rangle = \frac{1}{\hbar^2}[\mu^i_{0n}(\Delta\mu^j_{0n}\mu^k_{0n} + \Delta\mu^k_{0n}\mu^j_{0n})D^{(a)}_{nn} + \Delta\mu^i_{0n}\mu^j_{0n}\mu^k_{0n}D^{(b)}_{nn}] \quad (4)$$

is the theoretical expression in a two-level system. It is important to notice the influence of nondiagonal components of the dipolar transition moment between excited states: μ_{12}.[27] The dispersion factors D are given by

$$D^{(a)}_{nn} = \frac{{\omega_{0n}}^2 + 2\omega^2}{2({\omega_{0n}}^2 - 4\omega^2)({\omega_{0n}}^2 - \omega^2)}$$

$$D^{(b)}_{nn} = \frac{1}{2({\omega_{0n}}^2 - \omega^2)}$$

$$D^{(a)}_{12} = \frac{\omega_{01}\omega_{02} + 2\omega^2}{2({\omega_{01}}^2 - 4\omega^2)({\omega_{02}}^2 - \omega^2)}$$

$$D^{(a)}_{21} = \frac{\omega_{01}\omega_{02} + 2\omega^2}{2({\omega_{02}}^2 - 4\omega^2)({\omega_{01}}^2 - \omega^2)}$$

$$D^{(b)}_{12} = \frac{\omega_{01}\omega_{02} - \omega^2}{2({\omega_{01}}^2 - \omega^2)({\omega_{02}}^2 - \omega^2)} \quad (5)$$

Those expressions are of great relevance since they allow the evaluation of the dispersive contribution to the signal when the harmonic wavelength is close to the linear absorption wavelength. To compare with finite field calculations, which do not include dispersion, the SOS method was also extrapolated to $\omega = 0$.

The accuracy of the polarizability and hyperpolarizabilities SOS calculations are strongly dependent on both (i) the active space selected for the calculations and (ii) the method employed in deriving the ground and excited state properties.

As a rule, the active space in the present calculations consists of the highest occupied molecular orbital (HOMO) and the two lowest unoccupied ones (LUMO and LUMO+1) which are energetically degenerated in the C_3-symmetrical SubPcs.[28−30] This active space very well reproduces the electronic low-energy transitions of the SubPcs due to the breakdown of the Gouterman four level model observed in these compounds. Nevertheless, the expression for γ_{ijkl} in a three level model is appreciably complex, and only in the case of reduced symmetry the final expression is manageable. Molecular symmetry in the studied compounds is C_1 or C_3, which means that a mixed x, y, z character of the transitions is present and SOS calculations become rather tiresome. Thus, where recommended, we have approximated the theoretical treatment by a two-level model in order to calculate γ_{ijkl} under Kleinman symmetry conditions for a C_3 system. To optimize the computational effort that SOS

calculations imply, and in accordance with previous work in this field,[28−30] the permanent dipolar moments employed in the SOS calculations were obtained at semiempirical level by the INDO method[31] using the DFT optimized geometries.

***β*HRS and *γ*EFISH Calculations.** Using the tensor components of the molecular hyperpolarizabilities (β_{ijk} and γ_{ijkl}) obtained by SOS or FF procedures, it is possible to infer the contributions to the HRS and EFISH signals. In accordance with the molecular symmetry, the expressions for β_{HRS} and γ_{EFISH} are given by

$$\langle\beta_{HRS}^2\rangle_{C_3} = \frac{6}{35}\beta_{zzz}^2 + \frac{32}{105}\beta_{zzz}\beta_{zxx} + \frac{40}{105}\beta_{xxx}^2 + \frac{40}{105}\beta_{yyy}^2 + \frac{108}{105}\beta_{zxx}^2 + \frac{60}{35}\beta_{xyz}^2 \quad (6)$$

$$\langle\beta_{HRS}^2\rangle_{C_1} = \frac{6}{35}(\beta_{xxx}^2 + \beta_{yyy}^2 + \beta_{zzz}^2) + \frac{16}{105}(\beta_{xxx}\beta_{xyy} + \beta_{xxx}\beta_{xzz} + \beta_{yyy}\beta_{yxx} + \beta_{yyy}\beta_{yzz} + \beta_{zzz}\beta_{zxx} + \beta_{zzz}\beta_{zyy}) + \frac{38}{105}(\beta_{xyy}^2 + \beta_{xzz}^2 + \beta_{yxx}^2 + \beta_{yzz}^2 + \beta_{zxx}^2 + \beta_{zyy}^2) + \frac{16}{105}(\beta_{xxy}\beta_{yzz} + \beta_{xxz}\beta_{zyy} + \beta_{yyx}\beta_{xzz} + \beta_{yyz}\beta_{zxx} + \beta_{zzx}\beta_{xyy} + \beta_{zzy}\beta_{yxx}) + \frac{20}{35}(3\beta_{xyz}^2) \quad (7)$$

and the general expression for EFISH is given by

$$\gamma_{EFISH}(-2\omega;\omega,\omega,0) = \underbrace{\langle\gamma(2\omega;\omega,\omega,0)\rangle_{ZZZZ}}_{\gamma_{electronic}} + \underbrace{\frac{\langle\beta(2\omega;\omega,\omega)\rangle_{ZZZ}}{E_Z(0)}}_{\gamma_{orientational}} \quad (8)$$

where asuming Kleinman symmetry conditions

$$\langle\beta\rangle_{\Omega ZZZ}^{Kleinman} = \frac{\mu_0 E_Z(0)}{5kT}(\beta_{zzz} + \beta_{zxx} + \beta_{zyy}) \quad (9)$$

and

$$\gamma_{electronic}^{Kleinman} = \frac{1}{5}\sum_{i\neq j}^{x,y,z}(\gamma_{iiii} + \gamma_{iijj}) \quad (10)$$

In the case of the electronic contribution to the γ_{EFISH}, the expression for a C_3 symmetry gives

$$\gamma_{elec}^{C_3} = \frac{1}{5}[\gamma_{zzzz} + 2\gamma_{xxxx} + 4\gamma_{xxzz} + 2\gamma_{xxyy}] \quad (11)$$

These expressions will allow the comparison between theoretical and experimental results, as well as the determination of the relative strength of the electronic contribution to γ_{EFISH}.

Dipolar and Octupolar Hyperpolarizabilities *β*$^{J=1}$ and *β*$^{J=3}$. To quantify the dipolar and octupolar contributions to the NLO response of the studied compounds, we employed the two spherical components of β related to the dipolar and octupolar molecular anisotropy.[32] They represent the dipolar and octupolar contributions to the NLO response of the molecules. The expressions which defined them are, respectively, as follows:

$$||\beta^{J=1}||^2 = \frac{3}{5}(\beta_{xxx} + \beta_{xyy})^2$$

$$||\beta^{J=3}||^2 = \frac{1}{20}[3(\beta_{xxx} + \beta_{xyy})^2 + 5(\beta_{xxx} - 3\beta_{xyy})^2] \quad (12)$$

TABLE 1: Some Selected Geometrical Parameters for the SubPcs Considered in the Present Work

geometrical parameters	unsubst SubPc[a]	*m*-C_3 (1)	*m*-C_1 (2)	*o*-C_3 (3)	*o*-C_1 (4)
Bond Distances/Å					
B−Cl	1.934	1.914	1.914	1.914	1.914
B−$N_{pyrrole}$	1.484	1.488	1.488	1.491	1.491
$N_{pyrrole}$−C_α	1.381	1.380	1.380	1.379	1.380
C_α−C_β	1.457	1.457	1.457	1.459	1.459
N_{meso}−C_α	1.352	1.351	1.351	1.348	1.349
Bond Angles/deg					
Cl−B−$N_{pyrrole}$	113.0	113.4	113.4	113.3	113.3
$N_{pyrrole}$−B−$N_{pyrrole}$	105.8	105.3	105.3	105.4	105.4
Cα-Np−Cα	113.8	113.9	113.9	113.8	113.9
Cα-Nm-Cα	118.2	118.1	118.1	118.6	118.6
P_{phenyl}−P_{NO_2}		0	0	23	23, 25[e]
Indices of Pyramidality					
δ[b]/Å	0.70	0.69	0.69	0.71	0.71
$\delta_{B/Np}$[c]/Å	0.592	0.591	0.590	0.589	0.589
$d_{(Cl-Np)}$[d]/Å	2.768	2.853	2.853	2.854	2.853

[a] See ref 29. [b] $\delta = \Sigma(r_z)/28$, where r_z is the z coordinate of each atom of the molecule, the XY plane being defined by the three *meso* nitrogens. The summation runs over the 28 atoms of the SubPc's skeleton. The H and/or substituent atoms in peripheral positions as well as the axial halogen ligand were excluded. [c] Deviation of the B atom with respect to the plane determined by the pyrrole nitrogens. [d] Mean nonbonding distance between the Cl atom and the pyrrole nitrogens. [e] Two values are given due to the existence of two kinds of NO_2 groups in **4**.

The nonlinear molecular anisotropy ratio[4] ρ is then defined from the previous equations in the following manner:

$$\rho = \frac{||\beta^{J=3}||}{||\beta^{J=1}||} \quad (13)$$

whose values run from 0 (pure dipole) to ∞ (pure octupole).

Results and Discussion

Molecular and Electronic Structures. The DFT optimized structures of the trinitrosubphthalocyanines **1**−**4** have the strained pyramid-shape configuration that has been observed experimentally by X-ray diffraction.[33,34] The geometrical parameters obtained in the present calculations are in general agreement with those reported previously.[28−30] A representative selection of the calculated values may be found in Table 1, along with those corresponding to the unsubstituted SubPc.

Remarkably, the geometrical parameters corresponding to the heterocyclic isoindole units located within the SubPc core do not depend on the peripheral substitution pattern. It was previously demonstrated that, likewise, they do not depend on the nature of both the peripheral and the axial substituents.[35] Thus, it may be considered as a geometrical constant that characterizes the rigid core of the subphthalocyanines. Also, it is interesting to note that the B−Cl bond distance remains invariable for all the studied compounds (Table 1). This demonstrates that, in our case, the electron-withdrawing process is mostly inductive in nature since theoretical and experimental studies have shown that the B−Cl distance is correlated to the electron donor/acceptor properties of the peripheral substituents.[35]

The most significant structural difference among the series lies, not surprisingly, in the relative orientation of the nitro group with respect to the plane of the adjacent phenyl ring.[36,37] In the meta isomers **1** and **2** the nitro groups are coplanar to the phenyl ring whereas in the ortho isomers **3** and **4** the nitro groups are twisted ca. 23° with respect to the plane of the benzene groups

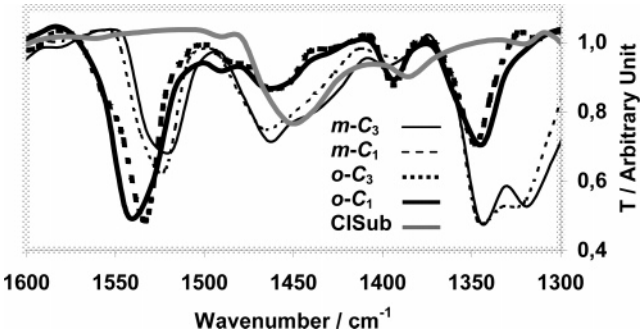

Figure 2. IR spectra of SubPcs **1**−**4** and unsubstituted chlorosubphthalocyanine in the region 1300−1600 cm^{-1}.

TABLE 2: Permanent Dipole Moments and Their Components for Compounds 1−4 from the B3LYP/6-31G(d,p) Calculation

	dipole moment (D)			
compounds	μ_x	μ_y	μ_z[a]	μ_{TOTAL}
***m*-C_3 (1)**	0.015	0.001	0.408	0.408
***m*-C_1 (2)**	2.874	−2.955	0.283	4.132
***o*-C_3 (3)**	−0.005	−0.011	−4.604	4.604
***o*-C_1 (4)**	−5.357	−5.727	−4.902	9.248

[a] The "z" direction corresponds to that of the B−Cl bond.

as a consequence of steric hindrance between the oxygen atoms of the NO_2 group and the meso nitrogen atoms of the subphthalocyanine in **3** and **4**. Moreover, a further twist is brought by nitro−nitro repulsion in SubPc **4** (see Table 1). Calculations showed that these repulsive interactions have direct consequences on the stability of the isomers. *o*-SubPcs **3** and **4** are more unstable than *m*-SubPcs **1** and **2** by about 15 kcal mol^{-1} as a consequence of the loss of conjugation experienced by the twisted NO_2 groups. On the other hand, two hypothetical structures of the ortho derivatives (referred to here as **5** and **6**) in which the nitro groups were constrained so as to stay coplanar to the adjacent benzene ring were shown to be less stable than SubPcs **3** ad **4** by ca. 15 kcal mol^{-1}.

Experimental evidence of the geometrical twist of the NO_2 groups in the ortho isomers comes from the IR spectra (Figure 2) of these isomers in which symmetric NO_2 stretching at 1310−1360 cm^{-1} dominates in the meta series (**1** and **2**) while asymmetric NO_2 stretching at 1490−1560 cm^{-1} dominates in the ortho series (**3** and **4**).

Table 2 shows the calculated permanent dipole moments of the studied compounds. As derived from these results, the peripheral electron-withdrawing nitro groups induce significant changes in the electron density distribution of the macrocycles with respect to both the unsubstituted and electron-donor substituted ones.[28] Thus, ***m*-C_3 (1)** has virtually null dipole moment along the *z*-axis because the electron-withdrawing effect of the apical Cl atom is exactly compensated for by that of the NO_2 groups located in the periphery (Table 2). As expected, in ***m*-C_3 (1)** and ***o*-C_3 (3)**, μ_x and μ_y were also shown to be virtually null as a consequence of the C_3 symmetric nature of the molecule. On the contrary, ***m*-C_1 (2)** and ***o*-C_1 (4)** were found to experience an increase of the *x* and y components of the dipole moments.

In contrast to unsubstituted and electron-donor substituted SubPcs,[28] the *z* components of the dipole moments of compounds **3** and **4** (Table 2) were found to be negative; the total negative charge concentrated at the NO_2 groups counterbalancing that of the apical chlorine atom. In the same way, the similarities in μ_z between, on one hand, compounds **1** and **2** and, on the other hand, compounds **3** and **4**, confirm that the distribution of the electron density is strongly determined by the inductive properties of the peripheral nitro substituents.

TABLE 3: Orbital Energies (in eV) for the Three Molecular Orbitals Included in the Three-Level Model Used in This Work To Calculate the NLO Properties of the Studied Compounds from the B3LYP/6−31(d,p) Calculations

	orbital energies/eV[a]			
compounds	HOMO	LUMO	LUMO+1	$\Delta E_{HOMO\rightarrow LUMO}$
***m*-C_3 (1)**	-6.456	-3.918	-3.918	2.538
***m*-C_1 (2)**	-6.457	-3.977	-3.832	2.480
***o*-C_3 (3)**	-6.237	-3.581	-3.581	2.656
***o*-C_1 (4)**	-6.219	-3.634	-3.436	2.585

TABLE 4: Experimental and Theoretical Values for β_{HRS} ($\times 10^{-29}$ esu)

		theor		
	expt β_{HRS}[a]	β_{SOS}[a]	β_{SOS}[b]	β_{FF}[b]
***m*-C_3 (1)**	9.2	19.6	3.6	4.8
***m*-C_1 (2)**	9.4	23.6	4.2	4.0
***o*-C_3 (3)**	10.4	14.5	3.1	4.0
***o*-C_1 (4)**	7.8	12.9	3.3	3.6

[a] Values for $\lambda = 1.34$ μm. [b] Values for $\omega = 0$.

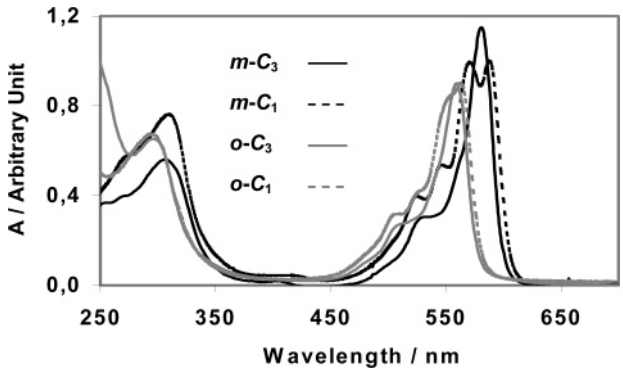

Figure 3. UV−vis spectra of SubPcs ***m*-C_3**, ***m*-C_1**, ***o*-C_3**, ***o*-C_1**.

Table 3 shows the calculated energies for the molecular orbitals included in the three level model used in the calculation of the NLO parameters, i.e., the highest occupied (HOMO) and the two lowest unoccupied (LUMO and LUMO+1) molecular orbitals. The energy difference (in eV) between the HOMO and LUMO is also included.

The electron transitions among these orbitals determine most of the features of the UV−vis spectra (Figure 3) of the studied compounds. The HOMO/LUMO gap is c.a 0.2 eV lower in meta isomers **1** and **2** than in the ortho ones **3** and **4**. Accordingly, UV−vis spectroscopy revealed an hypsochromic shift (ca. 30 nm) of the λ_{max} corresponding to the Q-band of compounds **3** and **4** with respect to that of **1** and **2** consistent with a loss of conjugation induced by the deviation of the NO_2 groups with respect to the plane of the phenyl rings. The nitro groups in compounds **1** and **2** are involved in the overall conjugation of the molecule, thus lowering the HOMO−LUMO energy gap with respect to SubPcs **3** and **4**. Moreover, the symmetry of these molecules is also reflected in their electronic absorption spectra by an acute splitting of the Q-band of the C_1 isomers as observed in Figure 3.

Experimental and Theoretical Nonlinear Optical Results. The experimental β_{HRS} values (Table 4) for all four isomers are rather similar and are comparable to those previously obtained with an analogous subphthalocyanine isomeric mixture,[11] showing the very little influence of the substitution pattern

TABLE 5: γ_{EFISH} ($\times 10^{-34}$ esu) Experimental and Theoretical Values for SubPcs 1−4

	expt	calculated SOS				calcd FF
	γ_{EFISH}[a]	γ_{EFISH}[a]	γ_{elec}[a]	γ_{orient}[a]	γ_{total}[b]	γ_{total}[b]
***m*-C_3 (1)**	−7.7	−2.5	−1.5	−1.0	−1.5	−1.7
***m*-C_1 (2)**	−9.0	−10.3	−2.2	−8.1	−6.1	−8.4
***o*-C_3 (3)**	17.9	6.6	−1.4	8.0	5.9	3.6
***o*-C_1 (4)**	11.6	9.8	−1.7	11.5	6.2	9.4

[a] Values for $\lambda = 1.9$ μm. [b] Values for $\omega = 0$.

TABLE 6: Dipolar and Octupolar Spherical Components and Molecular Anisotropy Ratio, ρ, for Compounds 1−4, As Calculated from Eqs 3−5, 12, and 13 in the SOS Formalism.

	***m*-C_3 (1)**	***m*-C_1 (2)**	***o*-C_3 (3)**	***o*-C_1 (4)**
$\|\beta^{J=1}\|^2$	0.4	11140	0.02	14040
$\|\beta^{J=3}\|^2$	306700	131510	61750	23620
r	840	3	1690	1

on the overall NLO response. This trend is further confirmed by the similarity between the (i) HOMO−LUMO energy differences (Table 3) and (ii) the SOS-derived $\gamma_{electronic}$ values (Table 5) between all four compounds.

The picture is rather different as far as the EFISH results are concerned (Table 5). The γ_{EFISH} experimental values are extremely sensitive to the substitution pattern at the periphery of the subphthalocyanine core and are also strongly correlated to the orientational contribution γ_{orient} to γ_{EFISH}. As observed in Table 5, γ_{EFISH} values depend on the permanent dipole moment of the molecule, and in particular on its component along the axis defined by the B−Cl bond. The correlation is such that sign reversal of the dipole moment value along the B−Cl axis induces a change of the sign of γ_{EFISH} at both theoretical and experimental levels.

The observed independence of the β_{HRS} values with respect to the substitution pattern at the periphery of the SubPc macrocycle may be understood as a signature of the dominant octupolar character of the subphthalocyanine core, as further confirmed by FF calculations. As seen in Table 6, both C_3-symmetrical SubPcs **1** and **3** present a strong octupolar character, with a weak $\beta^{J=1}$ dipolar component. For C_1-symmetrical SubPcs **2** and **4**, dipolar-to-octupolar ratio of the NLO response is close to unity, showing that especially for ***o*-C_1 (4)**, these molecules present a relatively smaller octupolar behavior. This is however expected, since ***o*-C_1 (4)** possesses the highest permanent dipole moment. Still, in all the four isomers the octupolar component is stronger than the dipolar one, confirming the robust octupolar character of all four SubPc isomers.

Conclusions

In conclusion, the modulation of the SubPc periphery by varying the substitution pattern allows the independent tailoring of dipolar and octupolar responses, and consequently the optimization of the performance and the processability. Controlled positioning of the nitro groups around the SubPc macrocycle allows the fine-tuning of the dipolar response without perturbing the robust octupolar contribution.

This fine control of the dipolar to octupolar contributions opens interesting perspectives for the use of multipolar NLO molecules in polymer-based polarization-independent electro-optic devices for telecommunication applications.[38,39]

Acknowledgment. This work was supported by (i) Ministerio de Educación y Ciencia (Spain) through Grants BQU2002-04697, BQU2001-0152, and PB98-0061, (ii) Comunidad de Madrid (Spain) through Grant 07N/0030/2002, and (iii) the European Union through Grant HPRN-CT-2000-00020. C.G.C. thanks the Ministerio de Educación y Ciencia for a "Ramon y Cajal" contract.

References and Notes

(1) *Handbook of Advanced Electronic and Photonic Materials and Devices*; Nalwa, H. S., Ed.; Academic: San Diego, CA, 2001; Vol. 9. *Nonlinear Optical Materials; Molecular Nonlinear Optics: Materials, Physics and Devices*; Zyss, J., Ed.; Academic Press: Boston, MA, 1994.

(2) Dalton, L. R.; Harper, A. W.; Ghosn, R.; Steier, W. H.; Ziari, M.; Fetterman, H.; Shi, Y.; Mustacich, R. V.; Jen, A. K. Y.; Shea, K. J. *Chem. Mater.* **1995**, *7*, 1060.

(3) Ledoux, I.; Zyss, J. *C. R. Phys.* **2002**, *3*, 407.

(4) Zyss, J. *J. Chem. Phys.* **1993**, *98*, 6583.

(5) (a) Senechal, K.; Maury, O.; Le Bozec, H.; Ledoux, I.; Zyss, J. *J. Am. Chem. Soc.* **2002**, *124*, 4560. (b) Wolff, J. J.; Siegler, F.; Matschiner, R.; Wortman, R. *Angew. Chem., Int. Ed.* **2000**, *39*, 1436.

(6) (a) Bartholomew, G. P.; Ledoux, I.; Mukamel, S.; Bazan, G. C.; Zyss, J. *J. Am. Chem. Soc.* **2002**, *124*, 13480. (b) Lambert, C.; Gaschler, W.; Nöll, G.; Weber, M.; Schämlzin, E.; Bräuchle, C.; Meerholz, K. *J. Chem. Soc., Perkin Trans. 2*, **2001**, 964. (c) Zhu, W.; Wu, G. *J. Phys. Chem. A* **2001**, *105*, 9568.

(7) (a) Sarkar, A.; Pak, J. J.; Rayfield, G. W.; Haley, M. M. *J. Mater. Chem.* **2001**, *11*, 2943. (b) Lee, W.-H.; Lee, H.; Kim, J.-A.; Choi, J.-H.; Cho, M.; Jeon, S.-J.; Cho, B. R. *J. Am. Chem. Soc.* **2001**, *123*, 10658.

(8) Claessens, C. G.; Torres, T. *J. Am. Chem. Soc.* **2002**, *124*, 14522.

(9) Claessens, C. G.; González-Rodríguez, D.; Torres, T. *Chem. Rev.* **2002**, *102*, 835.

(10) Martín, G.; Rojo, G.; Agulló-López, F.; Ferro, V. R.; García de la Vega, J. M.; Martínez-Díaz, M. V.; Torres, T.; Ledoux, I.; Zyss, J. *J. Phys. Chem. B* **2002**, *106*, 13139.

(11) Del Rey, B.; Keller, U.; Torres, T.; Rojo, G.; Agullo-Lopez, F.; Nonell, S.; Marti, C.; Brasselet, S.; Ledoux, I.; Zyss, J. *J. Am. Chem. Soc.* **1998**, *120*, 12808.

(12) Claessens C. G.; Torres, T. *Eur. J. Org. Chem.* **2000**, 1603.

(13) Claessens, C. G.; González-Rodríguez, D.; del Rey, B.; Torres, T.; Mark, G.; Schuchmann, H.-P.; von Sonntag, C.; MacDonald J. G.; Nohr, R. S. *Eur. J. Org. Chem.* **2003**, 2547.

(14) Terhune, R. W.; Maker, P. D.; Savage, C. M. *Phys. Rev. Lett.* **1965**, *14*, 681.

(15) Clays, K.; Persoons, A. *Phys. Rev. Lett.* **1991**, *66*, 2980.

(16) Zyss, J.; Chauvam, T.; Dhenaut, C.; Ledoux, I. *Chem. Phys.* **1995**, *177*, 281.

(17) Oudar, J. L. *J. Chem. Phys.* **1997**, *67*, 446.

(18) Kajzar, F.; Messier, J. *Rev. Sci. Instrum.* **1987**, *58*, 2081.

(19) Ward, J. F. *Rev. Mod. Phys.* **1965**, *37*, 1.

(20) Chopra, P.; Carlacci, L.; King, H. F.; Prasad, P. N. *J. Phys. Chem.* **1989**, *93*, 7120.

(21) Becke, A. D. *J. Chem. Phys.* **1993**, *98*, 5648.

(22) Lee, C.; Yang, W.; Parr, R. G. *Phys. Rev. B* **1988**, *37*, 785.

(23) Ditchfield, R.; Hehre, W. J.; Pople, J. A. *J. Chem. Phys.* **1971**, *54*, 724.

(24) Frisch, M. J.; Trucks, G. W.; Schlegel, H. B.; Scuseria, G. E.; Robb, M. A.; Cheeseman, J. R.; Strain, M. C.; Burant, J. C.; Stratmann, R. E.; Dapprich, S.; Kudin, K. N.; Millam, J. M.; Daniels, A. D.; Petersson, G. A.; Montgomery, J. A.; Zakrzewski, V. G.; Raghavachari, K.; Ayala, P. Y.; Cui, Q.; Morokuma, K.; Foresman, J. B.; Cioslowski, J.; Ortiz, J. V.; Barone, V.; Stefanov, B. B.; Liu, G.; Liashenko, A.; Piskorz, P.; Chen, W.; Wong, M. W.; Andres, J. L.; Replogle, E. S.; Gomperts, R.; Martin, R. L.; Fox, D. J.; Keith, T.; Al-Laham, M. A.; Nanayakkara, A.; Challacombe, M.; Peng, C. Y.; Stewart, J. P.; Gonzalez, C.; Head-Gordon, M.; Gill, P. M. W.; Johnson, B. G.; Pople, J. A. Gaussian98. Gaussian, Inc.: Pittsburgh, PA, 1998.

(25) Gosh, A. In *The Porphyrin Handbook*; Kadish, K. M., Smith, K. M., Guilard, R., Eds.; Academic Press: San Diego, CA, 2000; Vol. 7, p 1, and references therein.

(26) Gosh, A. *J. Porphyrins Phthalocyanines* **2000**, *4*, 380 and references therein.

(27) Maya, E. M.; Garcia-Frutos, E. M.; Vazquez, P.; Torres, T.; Martin, G.; Rojo, G.; Agullo-Lopez, F.; Gonzalez-Jonte, R. H.; Ferro, V. R.; Garcia de la Vega, J. M.; Ledoux, I.; Zyss, J. *J. Phys. Chem. A* **2003**, *107*, 2110.

(28) Ferro, V. R.; García de la Vega, J. M.; González-Jonte, R. H.; Poveda, L. A. *J. Mol. Struct. (THEOCHEM)* **2001**, *537*, 223.

(29) Ferro, V. R.; Poveda, L. A.; González-Jonte, R. H.; García de la Vega, J. M.; Torres, T.; del Rey, B. *J. Porphyrins Phthalocyanines* **2000**, *4*, 610.

(30) Ferro, V. R.; Poveda, L. A.; Claessens, C. G.; González-Jonte, R. H.; García de la Vega, J. M. *Int. J. Quantum Chem.* **2003**, *91*, 369.

(31) Anderson, W. P.; Edwards, W. D.; Zerner, M. C. *Inorg. Chem.* **1986**, *25*, 2728.
(32) Zyss, J.; Brasselet, S. *J. Nonlinear Opt. Phys., Mater.* **1998**, *7*, 397.
(33) Claessens, C. G.; Torres, T. *Angew. Chem., Int. Ed.* **2002**, *41*, 2561.
(34) Kietaibl, H. *Monatsh. Chem.* **1974**, *105*, 405.
(35) Ferro, V.; García de la Vega, J. M.; Claessens, C. G.; Poveda, L. A.; González-Ronte, R. H. *J. Porphyrins Phthalocyanines* **2001**, *5*, 491.
(36) Laerdahl, J. K.; Faegri Junior, K.; Romming, C.; Swang, O.; Mitgard, T.; Schoffel, K. *J. Mol. Struct.* **1998**, *445*, 89.
(37) Wilkins, A.; Small, R. W. H. *Acta Crystallogr., Sect. C: Cryst. Struct. Commun.* **1985**, *41*, 1509.
(38) Brasselet, S. Ph.D. Thesis, Orsay, France, 1997.
(39) Cazenobe, I. Ph.D. Thesis, Orsay, France, 1999.